Trans Indian Inst Met (June 2012) 65(3):265–273
DOI 10.1007/s12666-012-0130-0

TECHNICAL PAPER

Reduction of Nickel Oxide Powder and Pellet by Hydrogen

Ritayan Chatterjee · Sabyasachi Banerjee · Sayan Banerjee · Dinabandhu Ghosh

Received: 30 August 2011 / Accepted: 6 March 2012 / Published online: 13 April 2012

Abstract Reduction of nickel oxide (NiO) powder and pellet by hydrogen was studied in a thermogravimetric apparatus. The variables studied were temperature (573, 673, 773, 873, 973 K) and hydrogen flow rate (100, 150, 200 cc min^{-1}). With NiO powder 70–80 % reduction and with NiO pellets about 95 % reduction were achieved. With both NiO powder and pellets, the rate of reduction increased with increasing temperature and hydrogen flow rate and the linear nature of the fractional reduction versus time (F vs. t) plot, for the most part of the reduction at all temperatures, supported a rate control by gas film diffusion. The activation energies for the reduction of NiO powder and NiO pellet were found to be 20.14 and 19.21 kJ mol^{-1}, respectively. The SEM images showed that the grain size of nickel (Ni) produced was 1–2 μ, and the XRD analysis established the presence of Ni (and the absence of NiO) in the reduced sample.

Keywords Reduction kinetics · Nickel oxide · Thermo gravimetric apparatus · Gas film diffusion · Activation energy

1 Introduction

Nickel-based superalloys are required for superior creep strength in sophisticated aircraft applications. Development of commercially viable and environment-friendly processes toward the bulk production of functional materials like nickel and its many alloys require serious attention to meet the growing industrial needs. Metal oxides [1, 2] have wide technological applications, such as coating, catalysis, electrochemistry, optical fibers, sensors, etc. For the preparation of active oxide catalysts, the partial reduction of nickel oxide under hydrogen at elevated temperatures is the effective method [3–5]. Two different kinetic models have been proposed for the reduction of oxides: the "nucleation model" [4, 6] and the "interface-controlled model" [7]. The rate-limiting step of the reduction process in the 'nucleation model' is the generation of small aggregates of clusters of the new phase. On the other hand, in accordance with the 'interface-controlled model', the rate of metal oxide reduction is proportional to the surface area of the continuously reducing metal–metal oxide interface.

Hydrogen reduction of metal oxides is a promising process route with the possibility of using green energy and it represents a direct method for the preparation of metal powders with uniform composition. The kinetic study of the reduction of nickel oxide by hydrogen has been investigated by several researchers. Rodriguez et al. [8] found the correlation between the concentration of oxygen vacancies in the NiO lattice and the rate of oxide reduction. They confirmed that the reduction mechanism is controlled by the number of oxygen vacancies in the NiO lattice and by their migration from the bulk to the surface. The presence of oxygen vacancies has different potential energies so they have different absorption energies for hydrogen absorption, which leads to different activation energies. Richardson et al. [9] studied the hydrogen reduction of porous bulk NiO particles with in situ hot-stage X-ray diffraction (XRD) in the temperature range 448–573 K. The results obtained by these authors indicated that reduction by the dry reducing gas followed several steps: (1) an induction period associated with the initial reduction of NiO and the appearance of Ni metal clusters;

R. Chatterjee (✉) · S. Banerjee · S. Banerjee · D. Ghosh
Department of Metallurgical and Materials Engineering, Jadavpur University, Kolkata 700032, India
e-mail: ritayanchatterjee@gmail.com

(2) acceleration of the reduction rates as the size of the clusters increased; and (3) a pseudo-first-order process in which NiO disappeared and Ni appeared in concert until reduction slowed at a fractional conversion of about 0.8.

The first reported systematic measurement of bulk NiO reduction was by Benton and Emmett [10]. These authors measured water formation as an indication of the extent of reaction for a sample of NiO made by heating nickel nitrate at 673 K. They arrived at some very important conclusions and these are: (a) reduction occurs at the interface between NiO and previously reduced Ni; (b) there is an "autocatalytic" effect; (c) there is an induction (i.e. nucleation) period that depends on the nature of the sample and temperature; and (d) added water reduces the reduction rate and increases the induction period. Koga and Harrison [11] reviewed general reactions between solids and hydrogen and represented the induction process as generation of nickel atoms on the outer surface of NiO grains [11]. Bandrowski et al. [12] measured the water vapor produced during the reduction to generate sigmoidal conversion curves which they explained with a two-step kinetic model. The first step, which is the reaction between NiO and the hydrogen atoms adsorbed on NiO, predominates in the early part of the reduction and is proportional to the square root of the hydrogen pressure. The second step is the reaction at the metal-oxide interface between NiO and the hydrogen atoms adsorbed on the previously reduced NiO. The above models emphasized the mechanism and kinetics of the reduction process, but there was little uniformity in the physical properties of NiO grains and pellets used.

Utigard et al. [13] investigated the reduction kinetics of NiO granules formed by vapor deposition from a chloride solution, using thermogravimetry. They reported that in the temperature range from 673 to 873 K, the rate of reduction increased with increasing temperature and increasing hydrogen pressure. Microscopic analysis showed that in this temperature range the reaction followed the shrinking core model [13]. The same authors found that the activation energy for the reduction has a value of 90 kJ mol^{-1}, in the above temperature range. The kinetics of the isothermal reduction of nickel oxide, produced by the sol–gel procedure using hydrogen, was studied by the conventional and Weibull [14] kinetic analysis. The isothermal conversional method was used to find the dependence of the apparent activation energy and pre-exponential factor of reduction process on the fractional conversion of the reaction. The average value of the apparent activation energy was obtained as 100.7 kJ mol^{-1} [15]. The activation energies reported for the reduction of NiO by H_2 in separate studies vary from 20 [16, 17] to 101 kJ mol^{-1} [13, 15, 18, 19] in the temperature range 423–873 K.

The present paper intended to resolve the conflict in the activation energy values found in the earlier studies by undertaking the reduction of NiO, both in powder and pellet form, by hydrogen at different temperatures. Accordingly, the objective of the present work was to study the kinetics of reduction of NiO (powder and pellet) by hydrogen at varying flow rates (100–200 cc min^{-1}) in the temperature range 573–973 K in a thermogravimetric analyzer (TGA). In many previous studies, the powder bed would be shallow and the gas flow rate would be high enough to ensure chemically controlled reduction kinetics, but there could be some doubt about the requisite depth of the powder bed and the magnitude of the flow rate that would ensure a chemically controlled kinetics. Hence, in the present study, it was intended to find the rate controlling step from the variation of the fractional reduction vs time plot with temperature and flow rate. In addition, it was hoped that the results from NiO pellet reduction could be compared with those from the reduction of NiO powder to throw more light on the reduction kinetics and the rate controlling step. It was also intended to perform XRD and scanning electron microscope (SEM) studies of the reduced Ni for the purpose of phase identification and characterization of Ni powder, particularly its grain size.

2 Experimental

2.1 Preparation of NiO Pellets

NiO powder was taken in a watch glass. Double-distilled water was added to moisten the powder. The moistened mass was hand-rolled into a spherical shape. The green spherical pellet was then dried in an oven for 3 h in three equal stages from 373 to 573 K. The dried pellet was subsequently sintered in a horizontal resistance furnace (SiC heating elements) in oxygen atmosphere at 1273 K for 3 h. The sintered pellet was then used for the reduction experiment. The porosity (%) of the prepared pellet was obtained by using the relation: % porosity = 100 (theoretical density of NiO − apparent density of NiO pellet)/(theoretical density of NiO), where the apparent density of NiO pellet = (mass of the pellet)/(volume of the pellet). Typically, the mass of the pellet was 0.79 g and the diameter of the pellet was 0.992 cm, and hence the apparent density of the pellet was $0.79/(4/3\cdot\pi\ (0.992/2)^3) = 1.55$ g cc^{-1}; this gave the porosity of the pellet as 76.8 %, the theoretical density of NiO being 6.67 g cc^{-1}.

2.2 Experimental Procedure for the Reduction Experiments

The hydrogen reduction of NiO was carried out in a thermo gravimetric setup (make: Bysakh and Co., Model: Okay), which comprises a furnace, a balance (accuracy: 0.1 mg),

and an alumina crucible for holding the sample, as shown in Fig. 1. For experiments with NiO powder (Merck, Mumbai, 99.99 % purity, particle size: 2–3 μ), weights were taken between 123 and 131 mg. The powder sample was taken inside the alumina crucible which formed a shallow bed, while the (single) pellet was made to sit on the top of the crucible. The pedestal holding the crucible was then raised into the furnace, and the furnace was turned on and heated according to a suitable temperature–time program loaded into the system. As soon as the desired reduction temperature (isothermal) was attained, the reducing hydrogen gas was fed into the furnace (after a brief spell of argon purging to remove the residual air from the reduction chamber), and the reduction commenced. The hydrogen flow rate was monitored with the help of a flow meter (rotameter). The gas left the furnace through an exit port. The kinetics of pellet reduction was to be somewhat faster than powder reduction because of the easy access of the reducing gas in case of the pellet which, sitting on the top of the crucible, was freely exposed to the reducing gas stream. The reduction of the powder sample, on the other hand, relied upon the stagnant film of the reducing gas within the crucible formed by the reducing gas flowing over the crucible. The weight of the sample was displayed as a function of temperature at regular intervals (typically, 30 s) in the report generated by the system, giving the progress of the reaction. From the instantaneous weight of the sample the instantaneous fractional reduction (F) was found using the following relation:

$$F = \frac{\text{Mass of oxygen removed from the sample}}{\text{Initial mass of oxygen}}. \quad (1)$$

2.3 XRD and SEM Analysis

XRD analysis of the reduced sample was done to confirm the presence of Ni in the reduced sample. SEM study was made to identify the grain size and grain distribution of the Ni produced. The XRD and SEM studies were done with the reduced product obtained from the reduction of NiO powder and pellet each. The machines used were Rigaku Ultima 3, Japan for the XRD studies and Jeol 6360, for the SEM studies. The sample preparations were done by the conventional method.

3 Results and Discussion

3.1 Reduction of NiO Powder

In the study of reduction of NiO powder by H_2, the variables studied were reduction temperature (573, 673, 773, 873, 973 K) and flow rate of hydrogen gas (100, 150, 200 cc min^{-1}). The mass of the powder sample was kept nearly same at 123–131 mg in each experiment. About 70–80 % reduction was achieved.

3.1.1 Effect of Temperature

As can be seen in Fig. 2, the rate of reduction given by the slope of the F versus t plot generally increases with temperature in the temperature range 573–973 K, for the constant hydrogen flow rate of 100 cc min^{-1}. At each temperature, the F versus t plot is almost linear, clearly indicating a rate control by mass transfer (i.e., diffusion through the gas film made within the crucible by the overflowing hydrogen). The corresponding $1-(1-F)^{1/3}$ versus t plots, in Fig. 3 are all nonlinear, which reveals that the reduction kinetics was not controlled by the interfacial chemical reaction. Likewise, the $1-(1-F)^{2/3}-(2/3)F$ versus t plots in Fig. 4 are all, again, nonlinear, which reveals that the reduction kinetics was

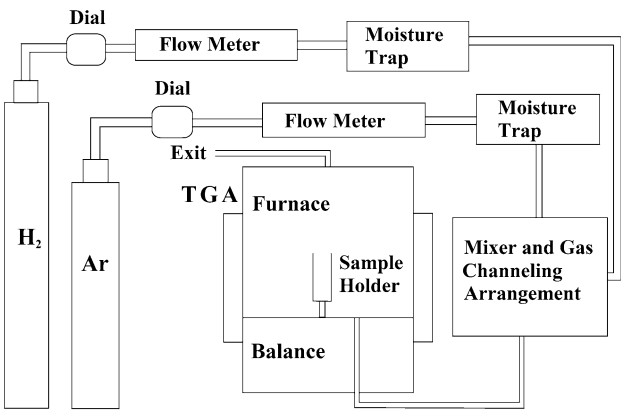

Fig. 1 Experimental set-up (TGA) for hydrogen reduction of NiO powder/pellet

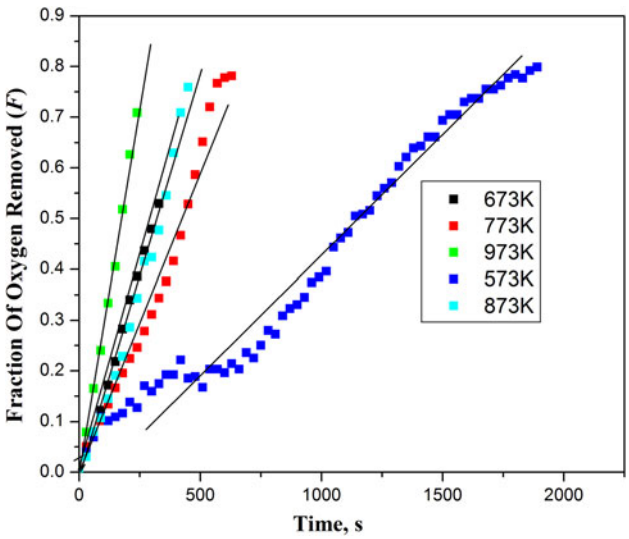

Fig. 2 F versus t plot for the reduction of NiO powder at different temperatures; hydrogen flow rate is 100 cc min^{-1}

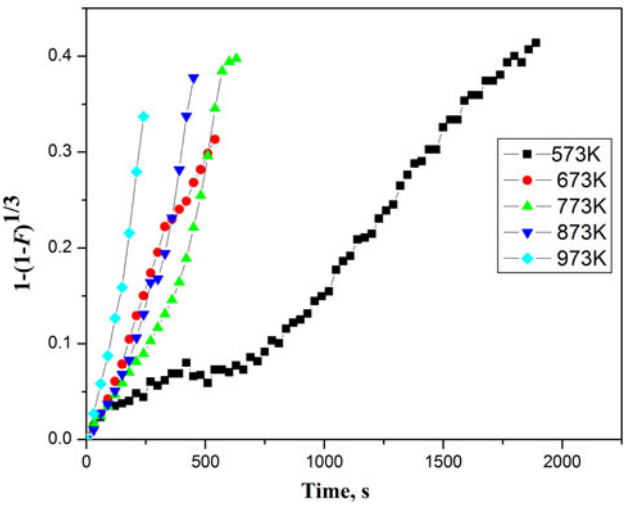

Fig. 3 $1-(1-F)^{1/3}$ versus t plot for the reduction of NiO powder at different temperatures; hydrogen flow rate is 100 cc min^{-1}

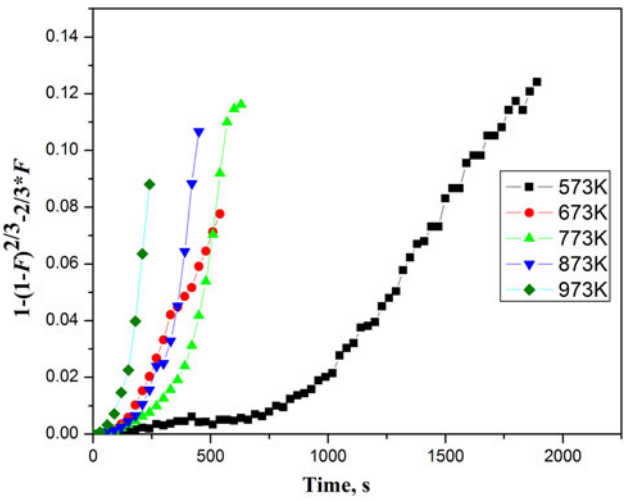

Fig. 4 $1-(1-F)^{2/3}-(2/3)F$ versus t plot for the reduction of NiO powder at different temperatures; hydrogen flow rate is 100 cc min^{-1}

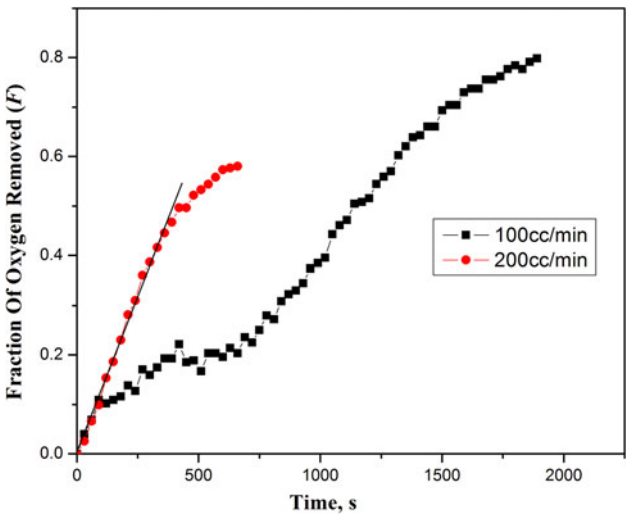

Fig. 5 F versus t plot for the reduction of NiO powder at different flow rates at temperature 573 K

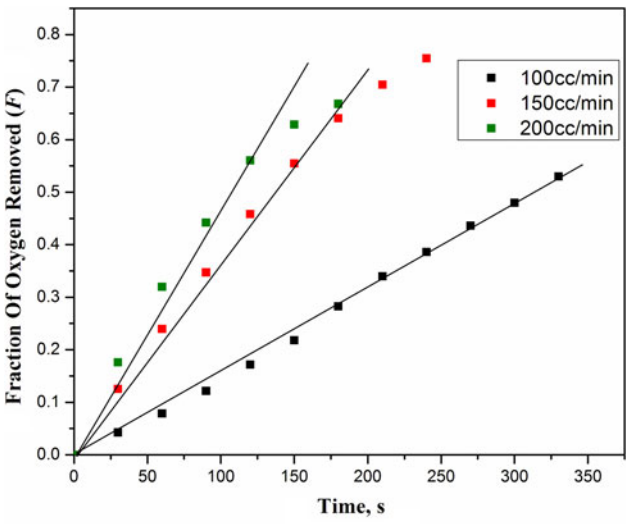

Fig. 6 F versus t plot for the reduction of NiO powder at different flow rates at temperature 673 K

neither controlled by the pore diffusion through the product (Ni) layer.

3.1.2 *Effect of Flow Rate*

The effect of hydrogen flow rate on the F versus t plot is shown for each of the five temperatures studied, namely, 573, 673, 773, 873, 973 K, in Figs. 5, 6, 7, 8, 9, respectively. There is a clear increase in the rate of reduction, given by the slope (dF/dt) of the plot, as the flow rate increases from 100 cc min^{-1} to 150 or 200 cc min^{-1}, particularly in the reduction regime from $F = 0$ to $F = 0.5 - 0.6$. This indicates that there was some difficulty of the reducing gas to have an access to the powder sample sitting well inside the crucible, mainly because of gas stagnation in the vertical crucible. With an increase in the flow rate of hydrogen, there was some renewal of the gas enclosed within the crucible. This helped in the removal of the product gas and increased the reducing potential of the reacting gas.

3.1.3 *Activation Energy Determination*

From the slope of the F versus t plot for each temperature in Fig. 2, the rate of the reaction is obtained. The rate constant k, which is the diffusivity ($D_{H_2-H_2O}$) in a diffusion-controlled kinetics, is proportional to the slope of the F versus t plot. The plot of ln k *vs* $1/T$ (T being the temperature of reduction), shown in Fig. 10, yields an activation energy of 20.14 kJ mol^{-1}. This small value of the

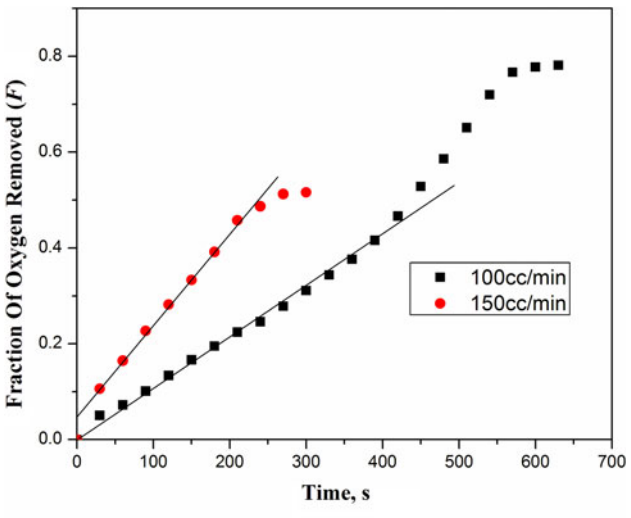

Fig. 7 *F* versus *t* plot for the reduction of NiO powder at different flow rates at temperature 773 K

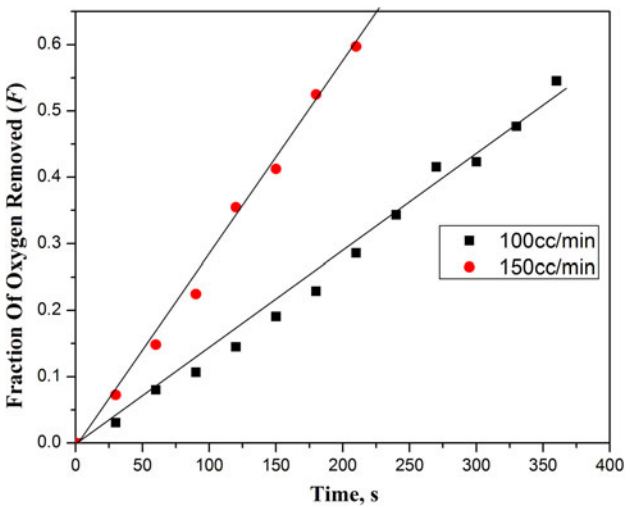

Fig. 8 *F* versus *t* plot for the reduction of NiO powder at different flow rates at temperature 873 K

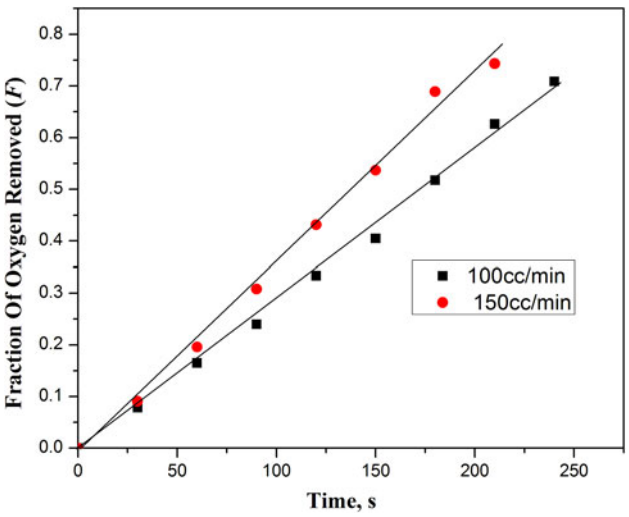

Fig. 9 *F* versus *t* plot for the reduction of NiO powder at different flow rates at temperature 973 K

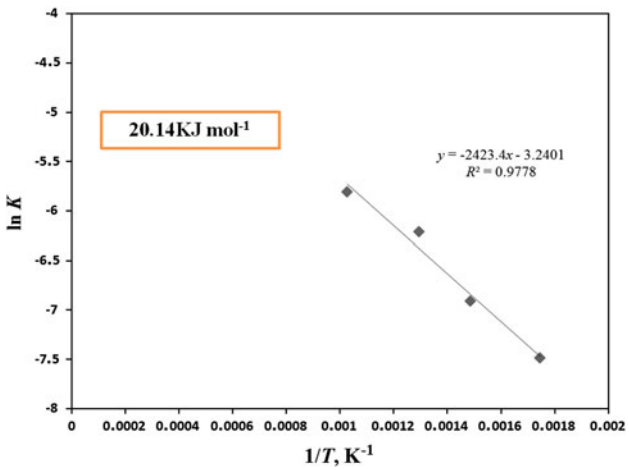

Fig. 10 Arrhenius plot for the determination of the activation energy for the hydrogen reduction of NiO powder

activation energy is characteristic of rate control by gas film diffusion.

3.1.4 SEM and XRD Studies

A SEM image of the reduced sample, given in Fig. 11, shows that the grain size of Ni produced is 1–2 μ, with the grains being elongated and uniformly distributed. There might have been some sintering of the grains. It may be noted that the particle size of the starting NiO powder was 2–3 μ. So it seems that the particles grew slightly finer upon reduction. In Fig. 12, the XRD analysis of the reduced sample shows (111), (200), (220), (311), (222) peaks all of which correspond to Ni. This supports the formation of Ni during the reduction.

3.2 Reduction of NiO Pellets

In the reduction of NiO pellets by hydrogen the variables studied were temperature (573, 673, 773, 873 K) and hydrogen flow rate (100 and 200 cc min^{-1}, at 873 K). It should be noted that each reduction run with pellet employed a single pellet with mass about 0.79 g and diameter about 0.99 cm. The maximum reduction of 95 % was obtained in the majority of cases. Characteristic plots for different rate controlling mechanisms, such as *F* versus *t* (for the gas film diffusion control), $1-(1-F)^{1/3}$ versus *t* (for the interfacial reaction control), and $1-(1-F)^{2/3}-(2/3)F$ versus *t* (for the pore diffusion control) are shown in Figs. 13, 14, 15.

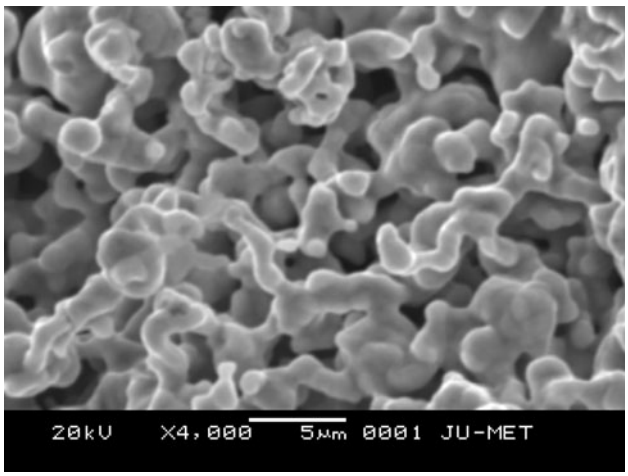

Fig. 11 Scanning electron microscope (SEM) photograph of Ni produced by the reduction of NiO powder

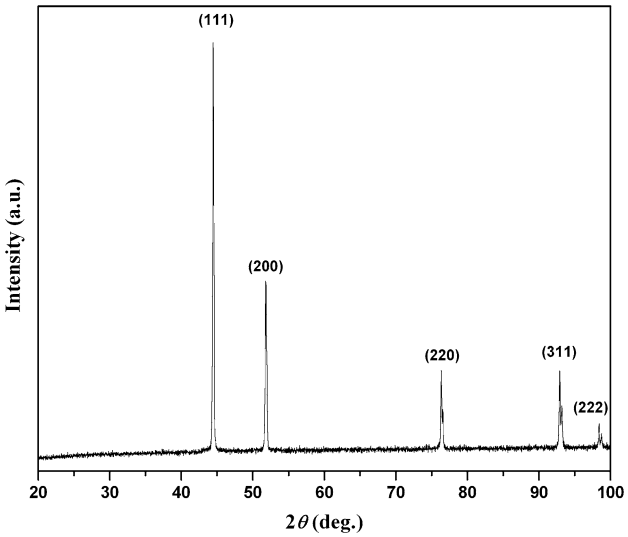

Fig. 12 XRD of reduced NiO powder showing the presence of Ni peaks

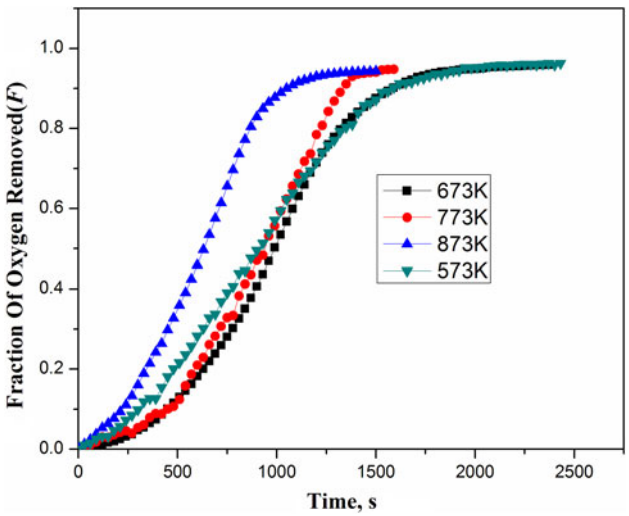

Fig. 13 F versus t plot for the reduction of NiO pellet at different temperatures; hydrogen flow rate is 100 cc min^{-1}

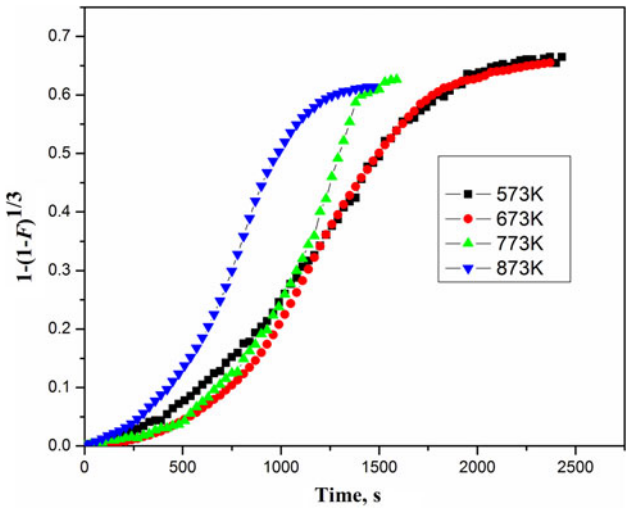

Fig. 14 $1-(1-F)^{1/3}$ versus t plot for the reduction of NiO pellet at different temperatures; hydrogen flow rate is 100 cc min^{-1}

3.2.1 Effect of Temperature

As can be seen from the F versus t plots of Fig. 13, the rate of hydrogen reduction of NiO pellet, which is given by the slope dF/dt of the plot, increases as the temperature increases from 573 to 873 K. The F versus t plots are typically a S-shaped curve which exhibits three distinct, consecutive regions. The initial incubation stage, characterized by a very slow rate, presumably represents the adsorption (chemisorption) of hydrogen on nickel oxide surface and the slow formation of nuclei of nickel. The middle-stage, characterized by a constant rate, is preceded by a short transition period during which the reaction accelerates rapidly, probably due to the autocatalytic effect of the nickel nuclei formed during the incubation stage. Notably, hydrogen adsorption on reduced nickel is much faster than on nickel oxide. Once the reduction rate reaches a maximum, it stabilizes and becomes virtually constant, resulting in a linear segment of the F versus t plot. It is of interest to note that the diffusivity $D_{H_2-H_2O}$ is proportional to the slope of the linear portion of the F versus t plot. The decaying stage, characterized by a gradually decreasing reduction rate, begins after a 90–95 % fractional reduction is achieved, depending on the temperature. Near the end of this stage, that is, in the proximity of complete reduction, even at high temperatures, the reduction remains a sluggish process which may be attributed to the entrapment of the unreduced nickel oxide grains by the growing metallic nickel clusters (nuclei) thereby rendering the residual oxygen virtually inaccessible to the hydrogen gas. It is

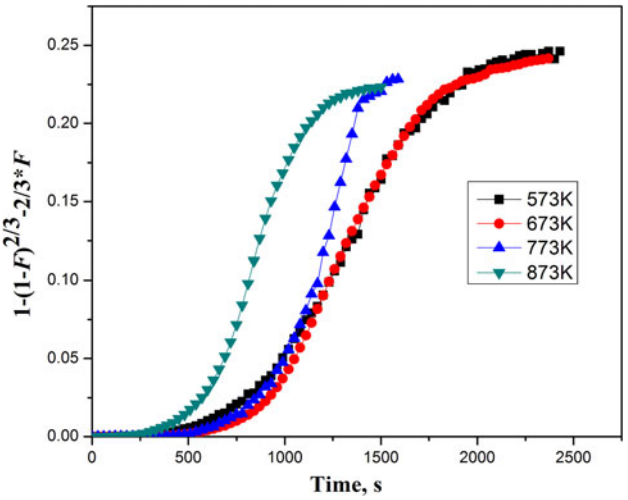

Fig. 15 $1 - (1 - F)^{2/3} - (2/3)F$ versus t plot for the reduction of NiO pellet at different temperatures; hydrogen flow rate is 100 cc min^{-1}

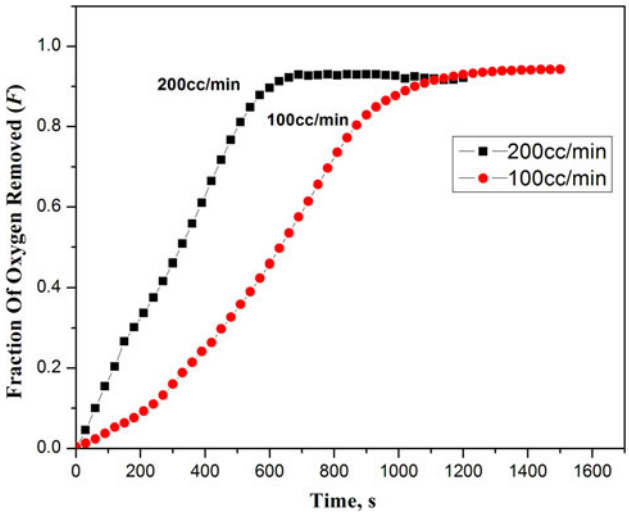

Fig. 16 F versus t plot for the reduction of NiO pellet at different flow rates at 873 K

likely that in the final stage, the reaction is governed by the diffusion of oxygen through the nickel.

It may be noted that the rate in the middle stage (which is the most predominant stage) in Fig. 13 is not so sensitive to temperature. It is expected that the rate in the middle stage, where the F versus t relation is linear, is controlled by gas film diffusion. However, this possibility is required to be further verified by the effect of the flow rate on the rate of reduction and the value of the activation energy. The plots of $1 - (1 - F)^{1/3}$ versus t and $1 - (1 - F)^{2/3} - (2/3)F$ versus t, in Figs. 14 and 15 are nonlinear and, hence, they do not support a rate control by interfacial reaction and pore diffusion, respectively.

3.2.2 *Effect of Flow Rate*

In Fig. 16, there is a clear enhancement of reduction rate as the hydrogen flow rate increases from 100 to 200 cc min^{-1} at 873 K. This supports a rate control by diffusion through gas film.

3.2.3 *Activation Energy Determination*

From the slope of the F versus t plot for each temperature in Fig. 13, the rate of the reaction is obtained. The rate constant k, which is the diffusivity $D_{H_2-H_2O}$ in a diffusion-controlled kinetics, is proportional to the slope of the F versus t plot. The plot of ln k versus $1/T$ (T being the temperature of reduction), shown in Fig. 17, yields an activation energy of 19.21 kJ mol^{-1}. This small value of the activation energy is characteristic of a gas film diffusion process. Notably, this activation energy found with the pellet reduction agrees very well with the activation energy (20.14 kJ mol^{-1}) obtained with the reduction of NiO

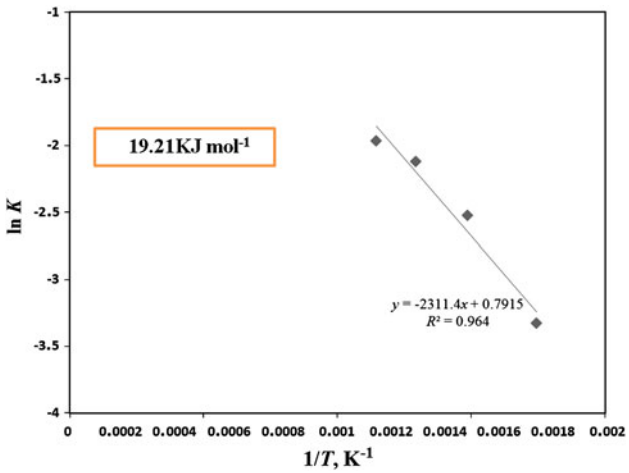

Fig. 17 Arrhenius plot for the determination of the activation energy for the hydrogen reduction of NiO pellet

powder and with the result (23 kJ mol^{-1}) of an earlier study [16]. This means that in the reduction of NiO by hydrogen, the rate of the interfacial reaction is quite fast even at the low temperatures (573–973 K) considered for the reduction, irrespective of pellets or powder samples. Likewise, there was not much resistance of the produced Ni layer on the fast kinetics of the reaction, presumably because the powder bed was sufficiently open and porous, or, in case of pellet reduction, the porosity of the starting NiO pellet was very high (76.8 %).

3.2.4 *SEM and XRD Studies*

A SEM image of the reduced pellet, given in Fig. 18, shows that the grain size of the Ni produced is around 1 μ, which is even smaller than that found with the reduction of

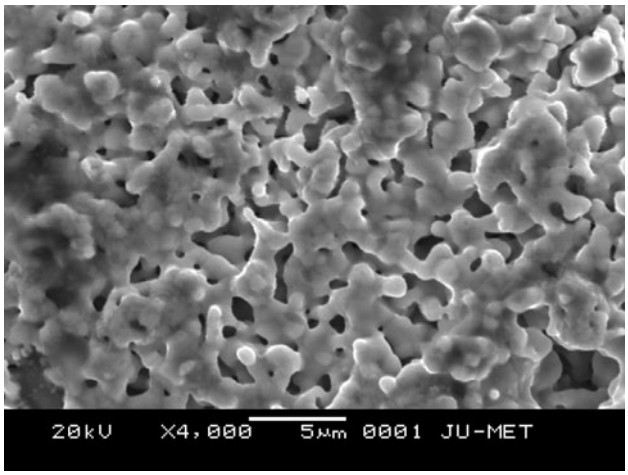

Fig. 18 Scanning electron microscope (SEM) photograph of Ni produced by the reduction of NiO pellet

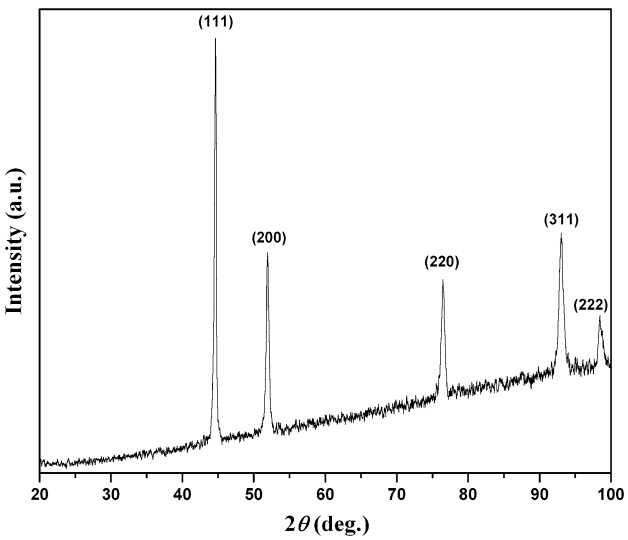

Fig. 19 XRD of reduced NiO pellet showing the presence of Ni peaks

NiO powder. In Fig. 19, the XRD analysis of the reduced pellet shows (111), (200), (220), (311), (222) peaks, which are the same as those shown (in Fig. 12) in case of NiO powder reduction. All peaks correspond to Ni, supporting the formation of Ni and elimination of NiO during the reduction.

4 Conclusions

In the present work, the kinetics of reduction of NiO powder and single NiO pellets by hydrogen was studied in a TGA. The variables studied were temperature (573, 673, 773, 873, 973 K) and hydrogen flow rate (100, 150, 200 cc min^{-1}). The mass of the powder samples varied in the range 123–131 mg and the mass of the single pellets varied in the range 790–956 mg. From the experimental results the following observations were made:

1. In the case of reduction of NiO powder, 70–80 % reduction was achieved and in the case of reduction of NiO pellets, about 95 % reduction was achieved.
2. With both NiO powder and pellets, the rate of reduction increased with increasing temperature and hydrogen flow rate.
3. The linear nature of the fractional reduction *vs* time (F vs. t) plot for the most part of the reduction of NiO powder/pellet at all temperatures supported a rate control by gas film diffusion.
4. The plot of ln k versus $1/T$ yields an activation energy of 20.14 kJ mol^{-1} for the reduction of NiO powder; a similar plot yields an activation energy of 19.21 kJ mol^{-1} for the reduction of NiO pellets.
5. The SEM images of the reduced sample showed that the grain size of Ni produced was 1–2 μ. The XRD analysis showed Ni peaks in the reduced samples.

Acknowledgments One of the authors, Ritayan Chatterjee, is with the Department of Metallurgical and Materials Engineering, Jadavpur University as a research fellow under U.G.C. research fellowship scheme. The financial support of the fellowship scheme is gratefully acknowledged.

References

1. Heinrich V E, and Cox P A, *The Surface Science of Metal Oxides*, Cambridge University Press, Cambridge (1994).
2. Pacchioni G, *Solid State Sci* **2** (2000) 161.
3. Delmon B, *Handbook of Heterogeneous Catalysis*, (ed) Ertl G, Knözinger H, and Weitkamp J, Wiley-VCH, New York (1997), p 264.
4. Furstenau R P, McDougall G, and Langell M A, *Surf Sci* **150** (1985) 55.
5. Lescop B, Jay J -Ph, and Fanjoux G, *Surf Sci* **548** (2004) 83.
6. Langell M A, *Surf Sci* **164** (1985) 543.
7. Delmon B, *Introduction á la cinétique hétérogéne*, chap. 11, Technip, Paris (1969).
8. Rodriguez J A, Hanson J C, Frenkel A I, Kim J Y, and Perez M, *J Am Chem Soc* **124** (2002) 346.
9. Richardson J T, Lei M, Turk B, Forster K, and Twigg M V, *Appl Catal A* **110** (1994) 217.
10. Benton A F, and Emmett P H, *J Am Chem Soc* **46** (1924) 2728.
11. Koga Y, Harrison L G, in *Comprehensive Chemical Kinetics*, (eds) Bamford C H, Tipper C F H, Compton R G, Elsevier, Amsterdam **21** (1984) p 120.
12. Bandrowski J, Bickling C R, Yang K H, and Hougen O A, *Chem Eng Sci* **17** (1962) 379.
13. Utigard T A, Wu M, Plascencia G, and Marin T, *Chem Eng Sci* **60** (2005) 2061.
14. Weibull W, *J Appl Mech* **18** (1951) 293.
15. Janković B, *J Phys Chem Solids* **68** (2007) 2233.

16. de Bokx P K, Labohm F, Gijzeman O L J, Bootsma G A, and Geus J W, *Appl Surface Sci* **5** (1980) 321.
17. Chatterjee R, Banerjee S, Banerjee S, and Ghosh D, *International Conference on Advances in Materials and Materials Processing 2011*, ICAMMP, Kharagpur (2011) p 29.
18. Janković B, Adnađevića B, and Mentus S, *Chem Eng Sci* **63** (2008) 567.
19. Janković B, Adnađevića B, and Mentus S, *Thermochimica Acta* **456** (2007) 48.